Eng. Research Bull.
Faculty of Eng. & Tech.,
Menoufia University.
Vol.VII Part II, 1985.

PP. 189-208 .

LOW CYCLE FATIGUE STRENGTH OF AL-1.5% Fe ALLOY

A. R. EL - DESOUKY*

ABSTRACT:

The increasing need for improved materials for high temperature applications has stimulated effort over the past two decades.
Low cycle fatigue (LCF, high stress and low numbers of cycles to failures) is an important consideration in the design of turbine components (disc and turbine blade) and for nuclear pressure vessels and piping tee-joint locations where the mixing of fluids at different temperatures may lead to cyclic stresses.

The purpose of this study is to present results of high temperature LCF measurements on an aluminium alloy containing 1.5% iron, in an attempt to use this alloy as a material for pistons and cylinder block in the engine HS 110 (850 HP & 12 cylinders) of the main battle tank AMX 30.

This alloy, when rapidly solidified, has shown to have an appropriate high temperature tensile strength in static testing in addition to high electrical conductivity.

Commercially pure conventionally cast aluminium was used for the purpose of comparison.

All tests were conducted at a nominal strain rate of 5×10^{-4} s^{-1} over a range of temperatures from ambient temperature to 400°C.

---

* Lecturer, Department of Design and Production Engineering, Faculty of Engineering and Technology, Menoufia University.

A comparison of LCF life of samples as expressed by the Coffin-Manson relation shows that Al-1.5% Fe alloy exhibited the best fatigue life.
Coffin-Manson parameters vary with the microstructure and deformation behaviour of the alloys.

The cumulative strain and the fatigue life were investigated under variable thermal and stress conditions.

NOMENCLATURE:

Δ_σ	Stress range (MPa)
$\Delta\varepsilon$	Total strain range
$\Delta\varepsilon_e$	Elastic strain component
$\Delta\varepsilon_p$	Plastic strain component
ε_f	Strain to failure
N_f	Number of cycles to failure
ε_n	Cumulative strain
σ_u	Ultimate tensile strength (MPa)
n/N_f	Ratio of fatigue life

INTRODUCTION:

Although historically fatigue studies have been concerned with conditions of service in which failure occured at more than 10^4 cycles of stress, there is a growing recognition of enginerring failures which occur at relatively high stress and low numbers of cycles to failures /1/. This type of fatigue failure must be considered in the design of many applications.

LCF conditions are frequently created where the repeated stresses are of thermal origin /2/. Since thermal stresses arise from thermal expansion of the material, it is easy to see that in this case fatigue results from cyclic strain rather than from cyclic stress.

LCF is a common form of fatigue testing which can be performed using either stress or strain control. The material response can be represented by hysteresis loops of stress range $\Delta\sigma$, versus strain range $\Delta\varepsilon$, and in many materials the first few cycles produce non-stabilised hysteresis loops which reflect the fluctuation of the Bauschinger effect in strain control tests, the stress range will either increase because of the hardening or decrease because of the softening of the material /3/. Fig. (1) illustrates a stress-strain loop under controlled constant strain cycling in a low cycle fatigue test /4/. In plotting $\Delta\varepsilon_p$ against N_f, the following relation-ship, often called Coeffin-Manson law, can be deduced:

$$\Delta\varepsilon_p \, N_f^b = C \quad \ldots \quad \ldots \quad \ldots \quad \ldots \quad \ldots \quad (1)$$

The exponent b depends on temperature and has a value between 0.5 and 1 /5/. The constant C can be evaluated by considering that the upper limit of LCF test is failure in the tension test, where:

$\Delta\varepsilon_p \cong \Delta\varepsilon_f = \ln\left(\frac{1}{1-q}\right)$ where q is the reduction of area. Taking N = 1/4 cycle & b = 1/2 ,

$$\rightarrow C = \varepsilon_f (1/4)^{1/2} = \varepsilon_f/2 \quad \rightarrow \Delta\varepsilon_p \, N_f^b = \varepsilon_f/2 = \tfrac{1}{2} \ln \frac{1}{1-q}$$

The elastic strain range is related to N_f by the relation /6/:

$$\varepsilon = \frac{\sigma_u}{E} N_f^c \quad \ldots \quad \ldots \quad \ldots \quad \ldots \quad (2)$$

Where, $c \cong -0.08$.

Since, $$\Delta\varepsilon = \Delta\varepsilon_e + \Delta\varepsilon_p = \frac{\sigma_u}{E} . N_f^c + \frac{\varepsilon_f}{2} N^{-b} \quad \ldots \quad (3)$$

The interesting aspect of the above equation is that it depends on only two structure-sensitive material properties: tensile strength and reduction of area.

Equations describing strain-life relationship at LCF can be expressed as follows /7/:

$$\Delta\varepsilon_p/2 = \varepsilon'(2N)^a \quad \text{/Coffin equation/} \quad \ldots (4)$$

$$\Delta\varepsilon_e/2 = (\sigma'/E)(2N)^b \quad \text{/Basquin equation/} \quad \ldots (5)$$

$$\Delta\varepsilon/2 = \varepsilon'(2N)^a + (\sigma'/E)(2N)^b \quad \ldots \quad \ldots \quad \ldots \quad (6)$$

Where ε' and σ' are coefficient of ductility and resistance to fatigue respectively.

The fatigue strength of metals decreases, in general, with increasing temperature. As the temperature is increased well above room temperature, creep will become important and at high temperatures (roughly greater than half the melting point) it will be the principal cause of failure.
Coffin /7/ has extended the analysis for LCF to consider the frequency dependence of high-temperature fatigue. Thus equation 1 becomes:

$$\Delta\varepsilon_p = C_2 N^{-b} \nu^{(1-k)b} \quad \ldots \quad \ldots \quad \ldots \quad \ldots (7)$$

Where ν is the frequency of stress application in cycle/min., and k is an exponent which measures the effect of frequency on fatigue life.

The purpose of this study is to present results of the effect of microstructure on LCF strength of aluminium. Commercially pure and aluminium containing 1.5% iron samples were used. The Coffin-Manson (strain-life) relation was applied.

EXPERIMENTAL PROCEDURE:

The alloy was prepared from highly pure Al and Fe. Commercial pure Al (99.67%), sample A, sand casted was used for comparison. The chemical composition of the

two samples is shown in Table 1.

	Fe	Si	Cu	Zr	Ti	Mn	V
A	0.25	0.07	0.001	0.002	0.001	0.001	0.001
B	1.5	0.079	0.003	0.003	0.002	0.004	0.003

Table 1: Chemical Composition in wt.%

Sample B was casted in a water-cooled copper mould (50 mmϕ) at a rate of cooling (measured at 3 , 5 mm from mould wall) of 45°C/S. Details information of the experimental technique was given elsewhere/9 & 12/.

The two samples were homogensied at 400°C for 6 hours. Fig. 2 shows the specimen configuration for LCF testing /10/. Test section of each LCF specimen was polished with sucessively finer grades of SiC paper to produce a surface finish of 0.5 µm or better, with finishing marks parallel to the logitudinal axis of specimen. After completing all machining operations, the specimens were degreased with trichlorethylene.

Static tensile testing was made at temperatures varying from 25 to 450°C on an universal Zwick machine at a cross head speed of the machine of 5 mm/min.

Fully-reversed push-pull LCF tests were carried out under total strain control on an Instron testing machine. The strain was controlled by a 10 mm Instron extensometer clamped to posts rigidly attached to the sample grips.

Thermal fatigue testing (change in temperature at constant machanical loading) was performed following the principal given by Coffin /11/.

All LCF tests were conducted at a nominal strain rate of 5×10^{-4} S^{-1} over a range of temperatures from ambient

temperature to 400°C.

Fig. 3. shows a block diagram of the test equipment which was developed to perform LCF tests under the above mentioned conditions, while Fig. 4 shows a view of the test equipment.
The specimens were induction heated and cooled by compressed air through nozzles at both sides of specimen.
Tests were conducted in air and no noticable oxide was found.

RESULTS AND DISCUSSION:

The mechanical properties at room temperature were shown in Table 2.

	σ_u MPa	H_v	δ%
A	130	170	5
B	250	230	12

Table. 2: Mechanical properties at room temperature.

δ is the elongation % measured in 5 cm gage length. The variation in mechanical properties of the two samples assisted the role of iron-addition and the fast rate of solidification. This can be attributed to a solid solution strengthening of Al-matrix, the finely dispersed Al_3Fe and the grain refinement effect /12/, as depicted metallography in Fig. 5.

Further, the benefits of refined and uniformly dispersed intermetallic compound for improving high temperature machanical properties have been shown in Fig. 6.

The metallographic examination of the fractured samples showed that sample B inhibited the dynamic recrystallisation process due to the presence of Al_3Fe in fine dispersed form. Even-through, the percent of strength recovered before recrystallisation is higher in B-sample, namely 35% compared with that for A-sample which come out to be about 10% only.
According to Cotteril & Mould /13/, the retardation can be explained as follows: the deformation structure consists of a uniform distribution of dislocations, without the regions of high lattice curvature that are required for the development of a new recrystallised grains.
In addition, fracture appearance changed from transgranular to intergranular with increasing temperature as shown in Fig. 7.

The cyclic hardening behaviour of samples A and B at constant total strain rate and at constant strain amplitude is shown in Fig. 8 for a range of temperature from 100 to 400°C. The stress values presented are the average of the tensile and compressive maxima for the particular hysteresis loops recorded. An apparent steady state in stress is achieved at all the temperatures investigated. The hardening curves, however, have qualitatively different shapes depending on temperature. At 100°C, the hardening curve consists of a rapid hardening with a rather abrupt change to a region with a lower hardening rate. In the neighborhood of 200-300°C the hardening rate decreases smoothly from an initial rate comparable with the initial rate at lower temperatures to a saturation value. At temperatures above 300°C the hardening curve has a local maximum so that the cyclic stress decreases toward the final saturation value.

Fe-addition to Al under rapid solidification condition (sample B) affected the hardening curve as depicted from Fig. 8.

Sample B-was characterised also by the existence of a peak in the hardening curve at temperatures $\geqslant$ 300°C. According to El-Desouky /12/ peaks in the flow curves represent the time necessary for generation and migration of vacancies to screw dislocations. It is quite possible that sample B has a higher concentration of vacancies due to the rapid rate of cooling and the high Fe-content. The role of vacancies has been considered to be due to the generation of friction stress during LCF and has been offered as an explanation for the linear temperature dependence associated with high temperature deformation /14/.

Fig. 9 gives a comparison of LCF of samples A & B, as expressed by the Coffin-Manson relation (strain-life curves). Sample B exhibited the best LCF life observed for the range of plastic strain studied. Recent results /15/ indicate that structures which reduce inhomogeneous deformation in the alloys are more resistant to fatigue. This may explain the increases in LCF life of sample B (compared with A) since it has a refined grain structure and a well-known means of promoting homogeneous deformation is a reduction in grain size.
Also, the refined grain structure of sample B reduces dislocation pile-ups and resultant stress concentrations at grain boundaries leading to increased ductility and an overall homogenisation of deformation. Selines /16/ observed a similar improvement in LCF life of Al-alloy 7075 (1.5 % Mg, 5.5 %Zn) and was attributed to an increase in fracture toughness.
However, fracture toughness is related to critical crack growth resistance, and is not necessarily adequate for predicting fatigue resistance /15/. We believe that the improved LCF life for sample B is more probably related to an improved homogenity of deformation.

The effect of stress range $\Delta\sigma$ on the relationship between ε_n and n/N_f at 200°C is shown in Fig. 10. On

the other hand, Fig. 11, shows the variation of ε_n with n/N_f under thermal-cyclic conditions (at constant mean stress). A comparison between these two figures clearly demonstrates the intensive effect of temperature (thermal cyclic) rather than stress range on ε_n.

The hardening and softening processes can be followed from $\Delta\varepsilon_p / \Delta\varepsilon_e$ vs. n/N_f curve under thermal fatigue cycling condition (Fig. 12). The decrease in $\Delta\varepsilon_p / \Delta\varepsilon_e$ can be attributed to strain hardening in which the rate of strain acumulation decreases also. This is followed by equilibrium stage between hardening and softening processes, while the latter stage is characterised by a rapid increase in $\Delta\varepsilon_p / \Delta\varepsilon_e$ towards fracture. This increase can be mainly due to crack-initiation and -propagation rather than to softening processes.

CONCLUSIONS:

The results of low cyde fatigue (LCF) experiments at a constant strain rate over a range of temperatures from ambient temperature to 400°C are reported for aluminium alloy containing 1.5 % iron rapidly solidified (sample B) and a conventionally cast commercially pure aluminium (sample A) for the purpose of comparison.

Several findings are of interest.

1) The cyclic hardening curves change shape with increasing temperature, developing a maximum in the cyclic hardening behaviour for sample B at higher temperatures.

2) A comparison of LCF life of samples A & B as expressed by the Coffin-Manson relation shows that sample B exhibited the best LCF life observed for the range of plastic strain studied.
   The improvement in LCF resistance attained for sample B is due to the improved homogenity of deformation

(as a result of grain refinement effect) which delayed crack initiation and failure.

3) Cumulative strain versus fatigue life ratio for isothermal - and thermal - tests shows a similar dependance as in creep conditions.
The existance of the three stages, namely: hardening, steady state and accelerated softening, depends on the interaction between stress and temperature.

4) These results indicate that the proper control of grain structure is a potential in the development of fatigue-resistant Al-alloys.

ACKNOWLEDGMENT:

The work described in this paper was sponsored by: Maintenance Corps, Ministry of Defence and Aviation, Saudi Arabia and was performed at the Main Tanks Workshop, Taif.
With profound gratitude and deep-felt respect, I thank Major General: Murshed A. El-Ammari for his meticulous, critical and generous assistance.
My deep appreciation is extended to Prof. Dr. A. A. Nasser for his frank, candid and constructive contribution.

REFERENCES:

1) L. F. Coffin, Jr., Met, Eng. Q., V3 (1963) 15.

2) S. S. Manson, "Thermal Stresses and Low Cycle Fatigue", McGraw-Hill Book Company, NY (1966) 124.

3) J. C. Tsou, "Low Cycle Fatigue Response of Polycrystalline Al", Ph.D. Thesis University of Rochester (1982) 145.

4) "Manual on Low Cycle Fatigue Testing", ASTM Spec. Tech. Publ. (1969) 465.

5) A. Coles and A. Chitty: Proc. Int. Conf. on: "Thermal and High-Strain Fatigue", London (1967) 328.

6) S. S. Manson: Exp. Mech. 5 (7) (1965) 193.

7) L. F. Coffin, Jr., "Fatigue at high temperature" ASTM Spec. Tech. Publ. 520 (1973) 5.

8) L. F. Coffin, Jr., Proc. Air Force Conf. Fatigue and Fracture Aircraft Structures and Material AFFDL TR. 70-144, Sept. (1970) 301.

9) A. A. Nasser, A. R. El-Desouky and S. M. Serag, Eng. Bul. of Monofia University VIII, Part II (1979) 199.

10) Recommend Test Procedure for LCF Testing of Metallic Material below Creep Range" prepared by ASME Subgroup on Fatigue Strength, June (1973).

11) L. F. Coffin, Jr., Trans. ASME, August (1954) 931.

12) A. R. El-Desouky, "Effect of Structural Conditions on Hot Workability and Electrical Conductivity of Al-Alloys" Dr. Eng. Thesis, Bergakademie Freiberg, (1977).

13) P. Cotterill and P. R. Mould, "Recrystallisation and Grain Growth in Metals", Surrey Univ. Press, London (1976).

14) S. P. Bhot and C. Laird, Fatigue Eng. Mater. Struct., 1 (1979) 59.

15) D. S. Thompson and R. E. Zinkham, Research on Synthesis of High Strength Al Alloys, AFML Tech. Rep. TR-84-128, Part I, December (1984).

16) R. J. Selines, Ph.D. Thesis, Massachusetts Inst. Technol., Cambridge, Mass., (1974).

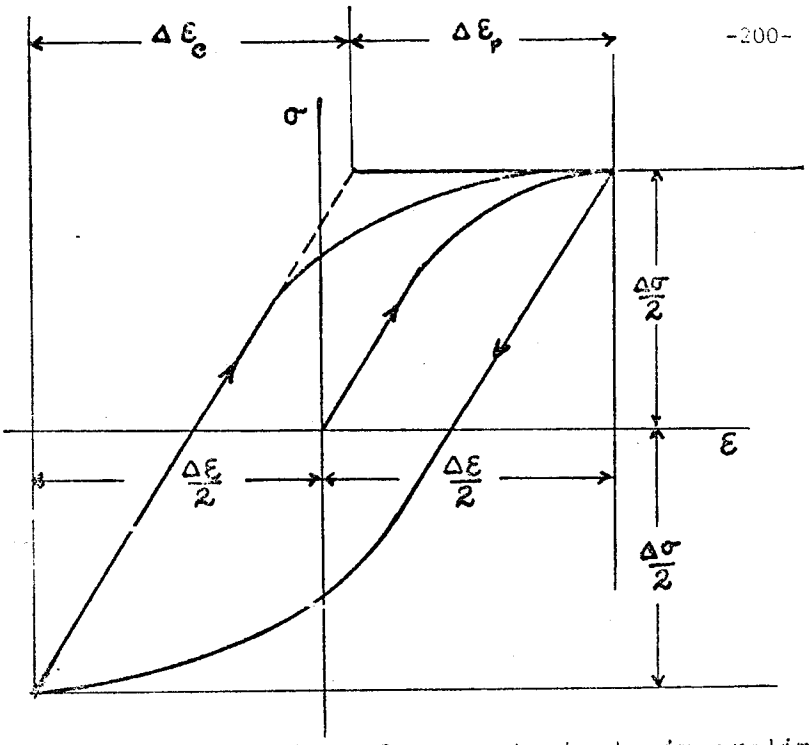

Fig. 1 : Stress - Strain loop for constant strain cycling

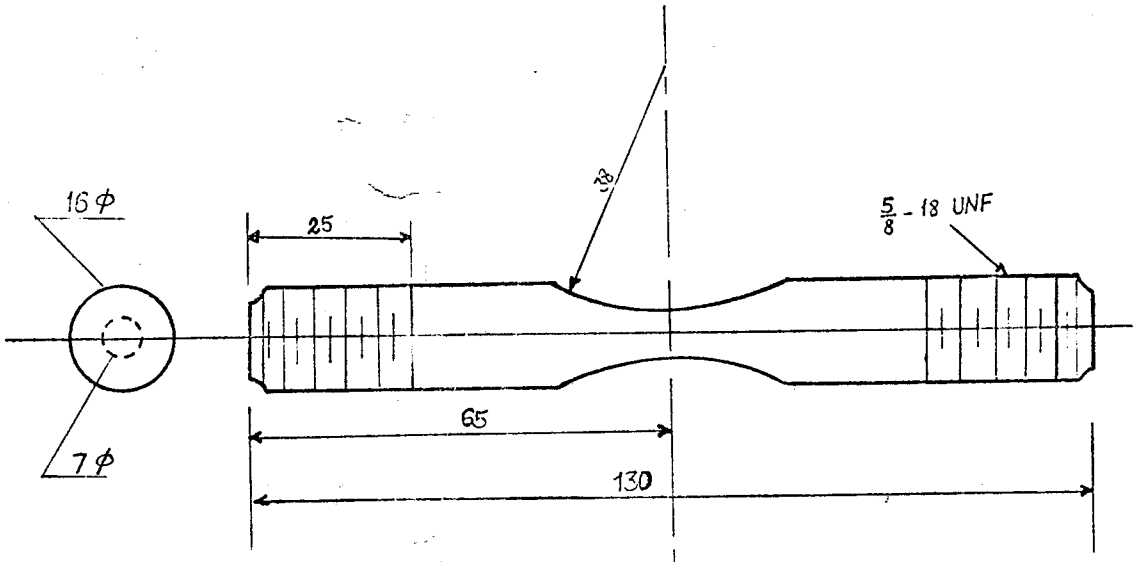

Fig. 2 : Specimen Configuration

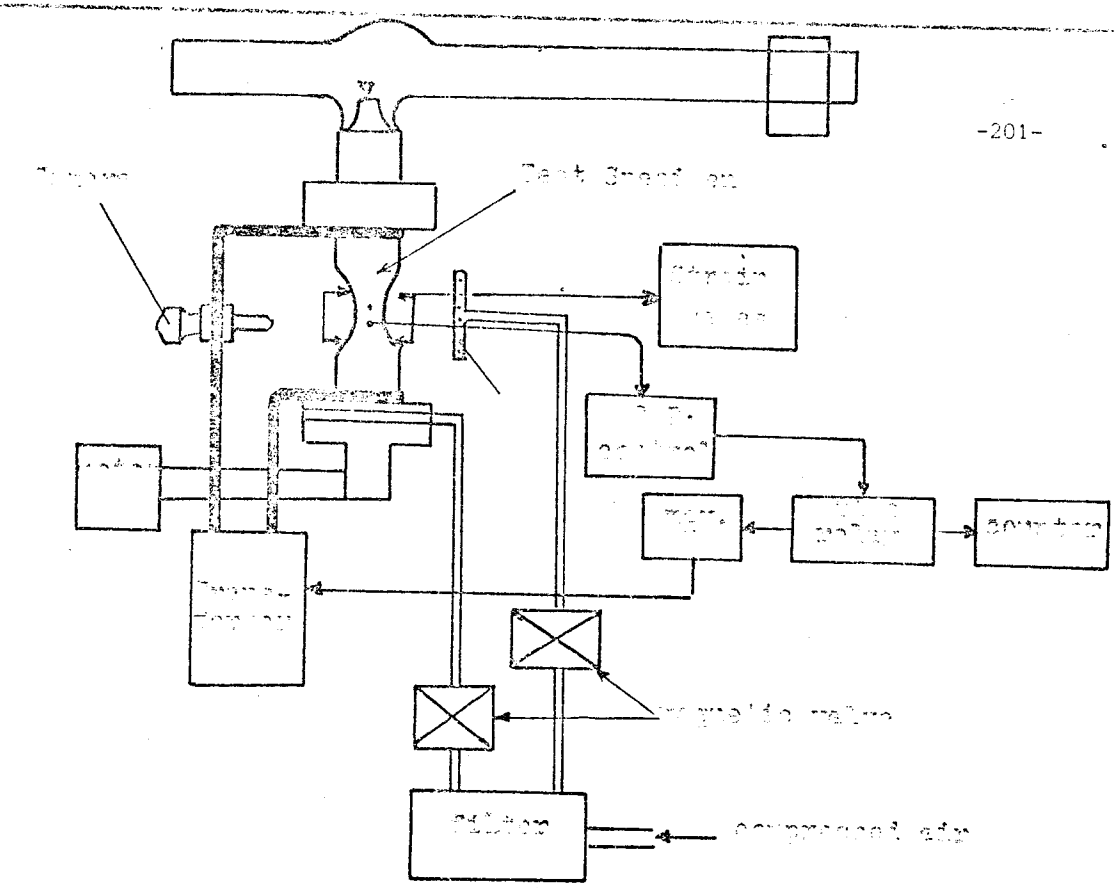

Fig.3 Block diagram of test equipment

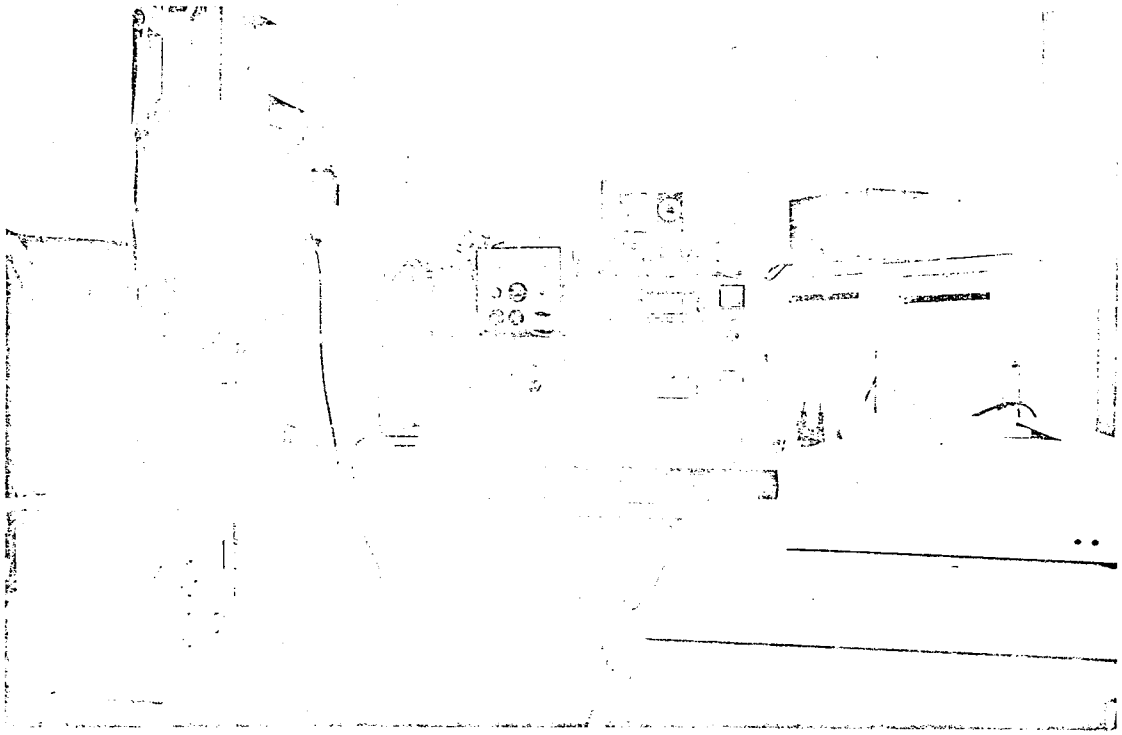

Fig 4 Test Equipment

Ag 337/74/0505

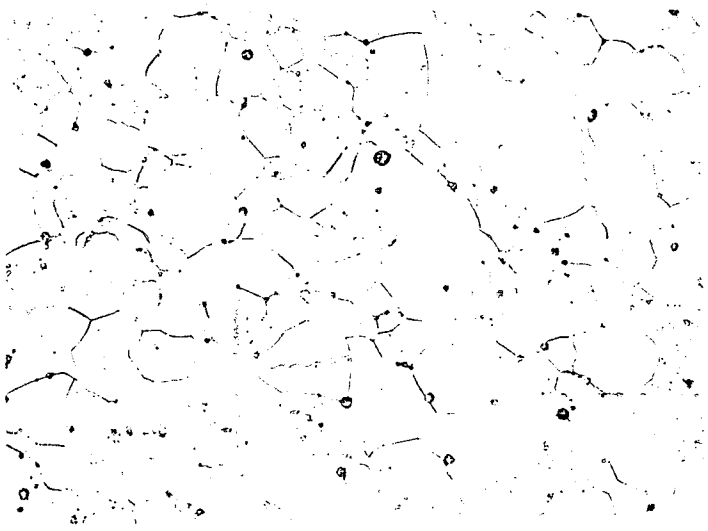

Sample A

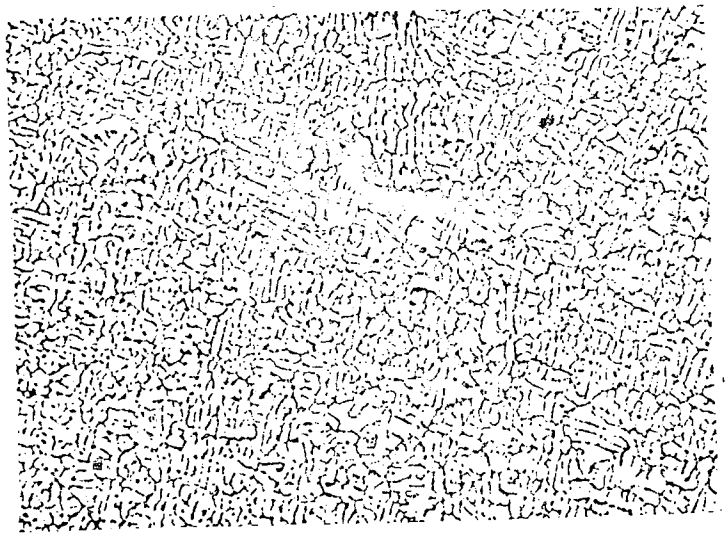

Sample B

Fig.5 Microstructure in the as-cast condition (200 X)

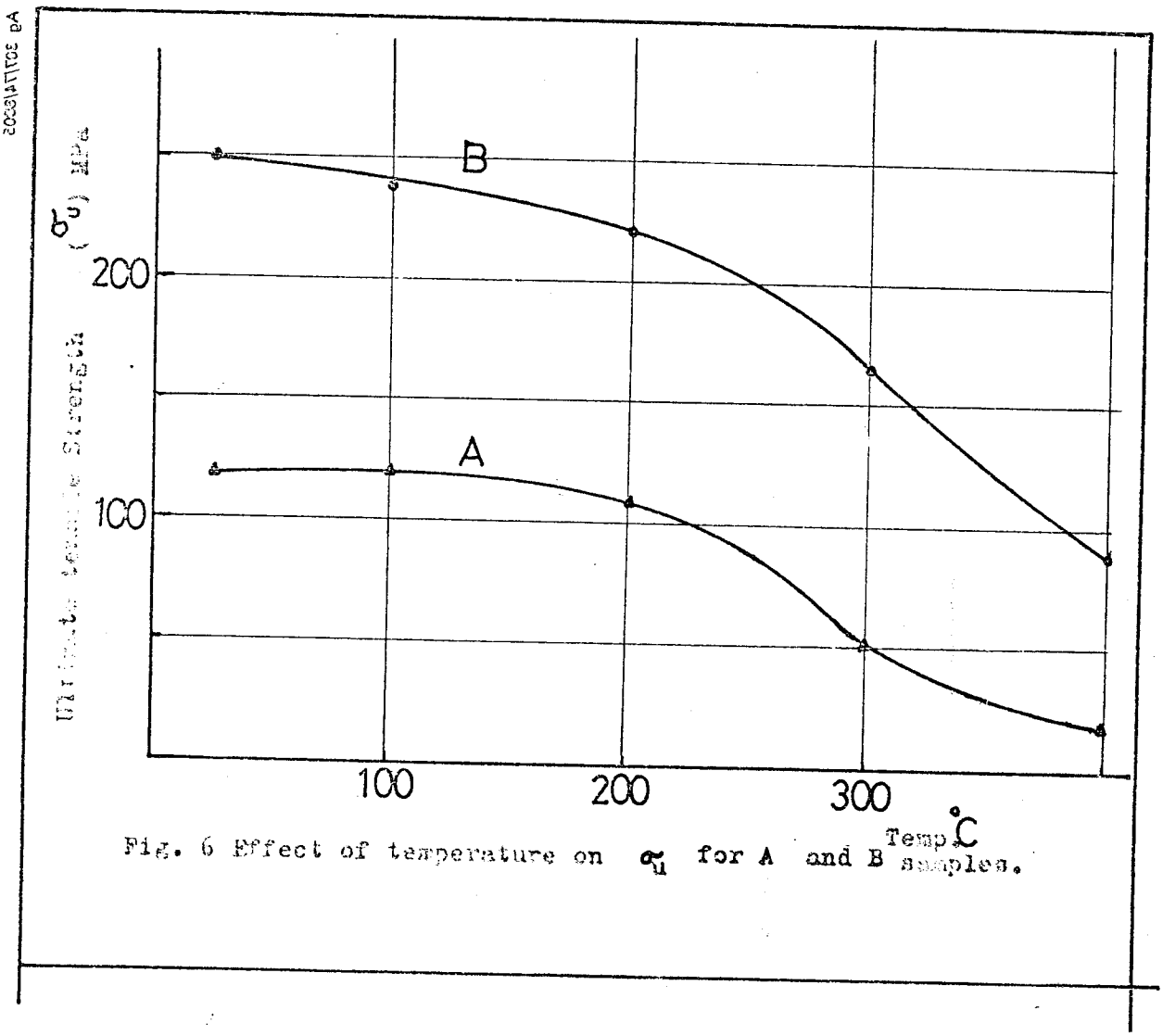

Fig. 6 Effect of temperature on σ_u for A and B samples.

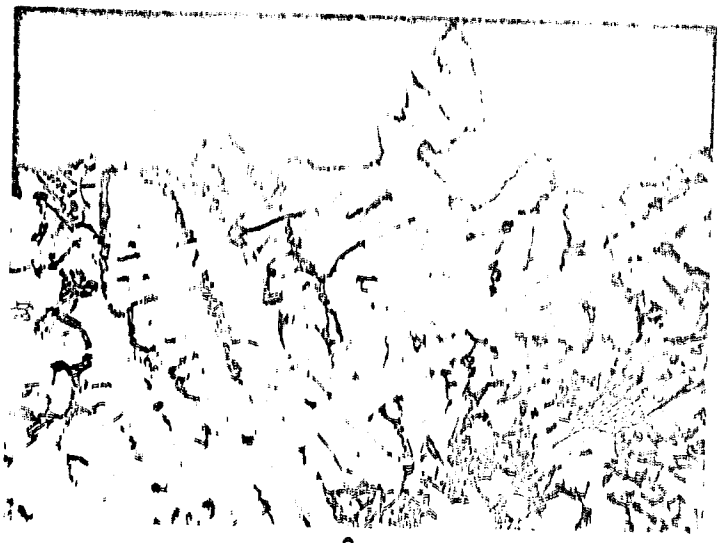

200 °C

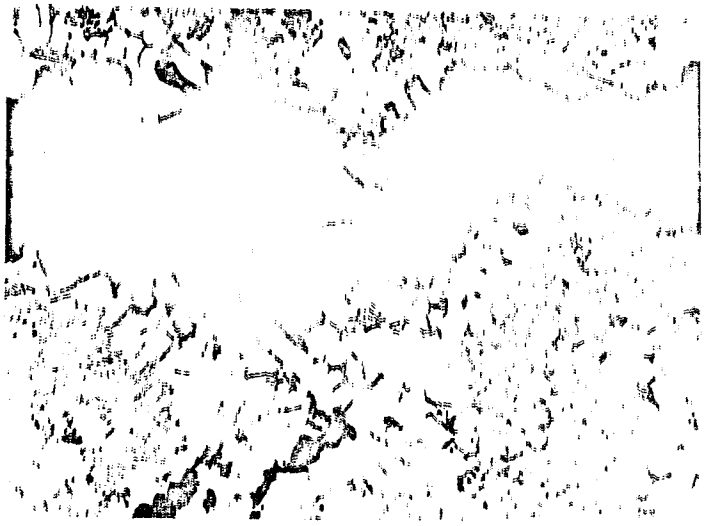

400 °C

Fig.7 Fracture appearance of sample 3 at 200 & 400 °C tensile testing temperatures (400 X).

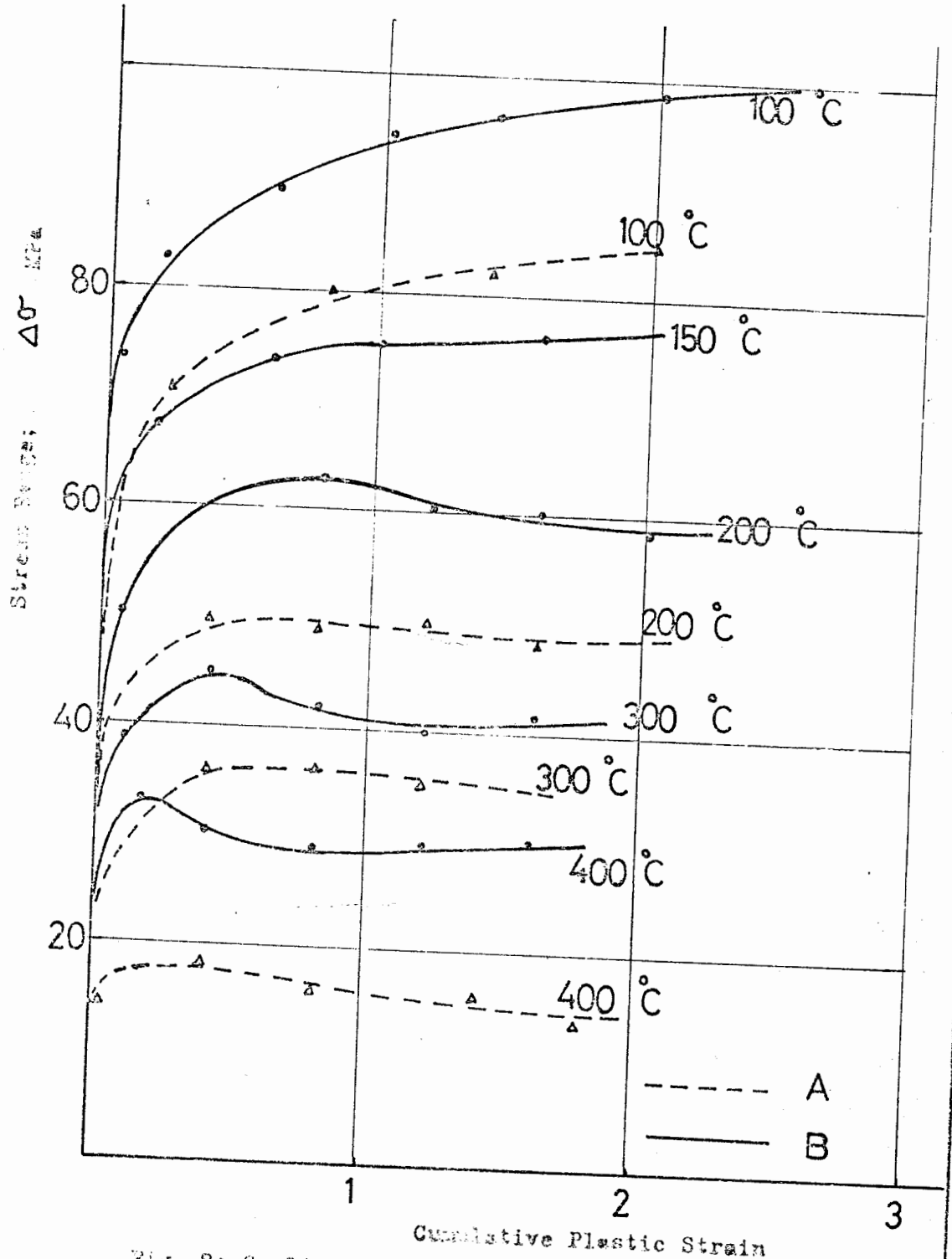

Fig. 8: Cyclic hardening curves at high temperatures
($\Delta\varepsilon$ and strain rate are constants)

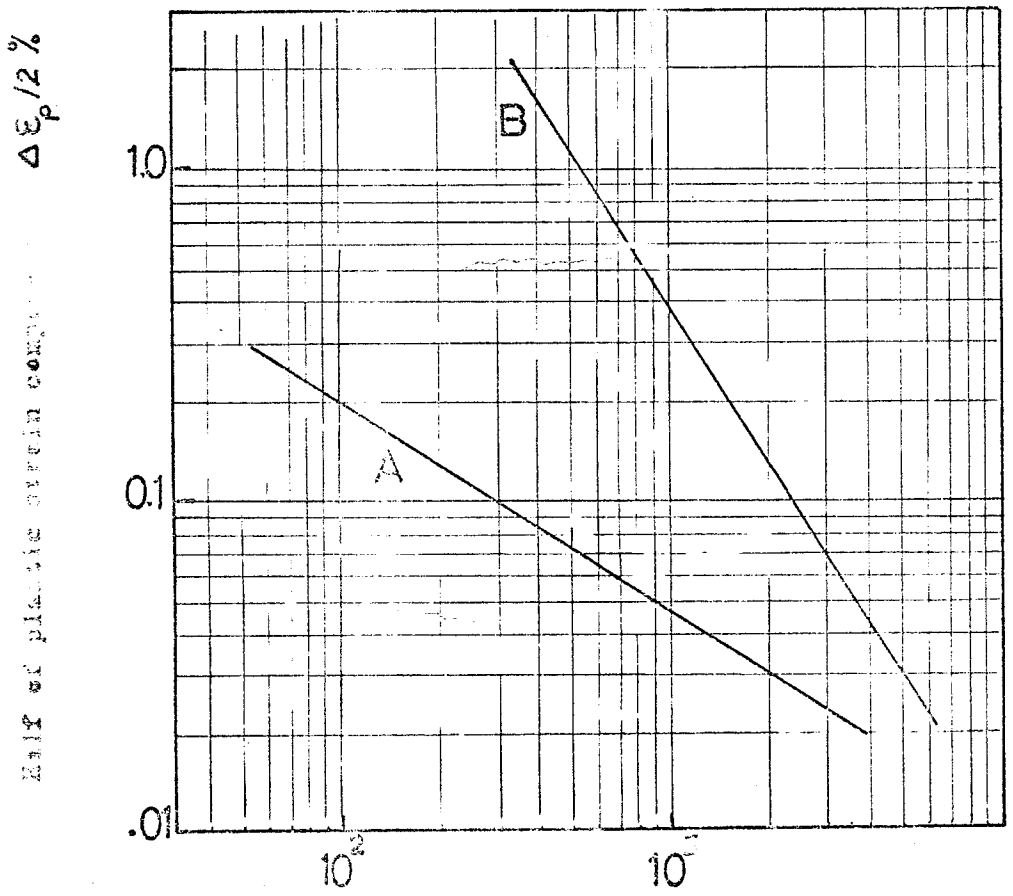

Fig. 9: Strain-life (Coffin-Manson) Curves of A , B Steples

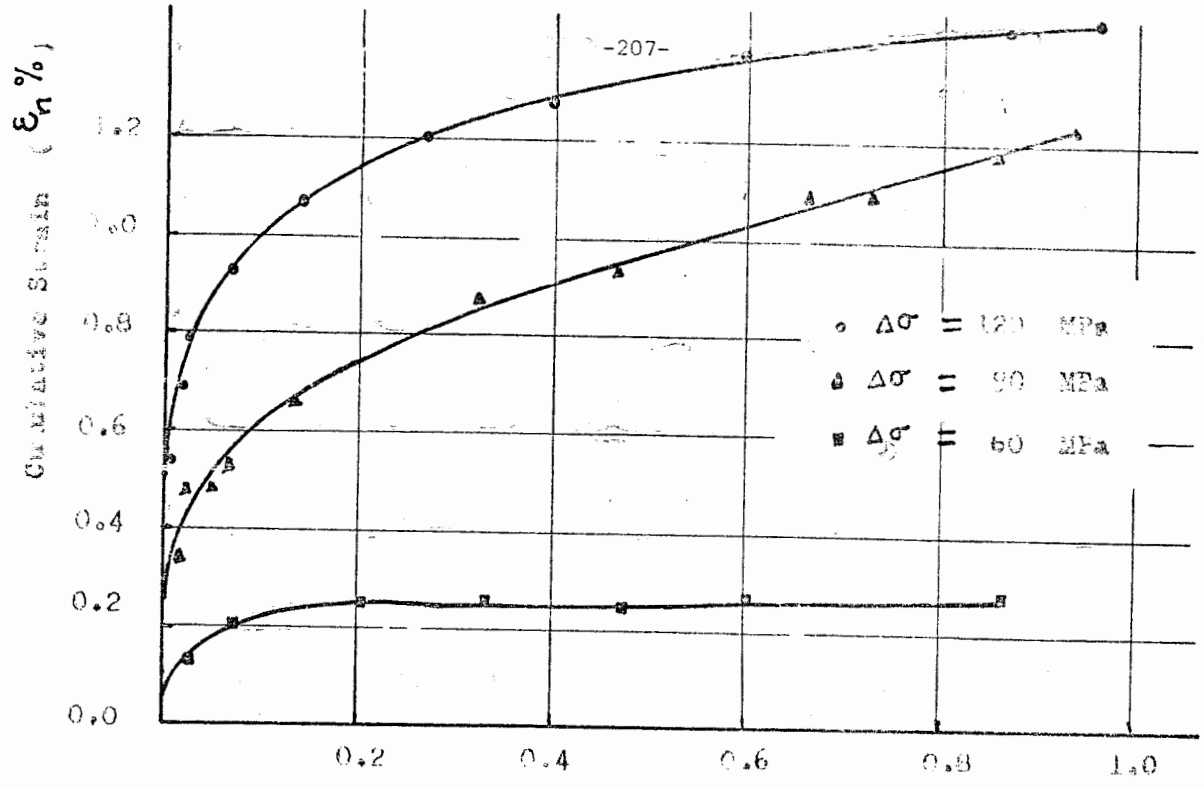

Fig.10 Effect of $\Delta\sigma$ on ε_n vs. n/N_f at 200 °C , B.Samples

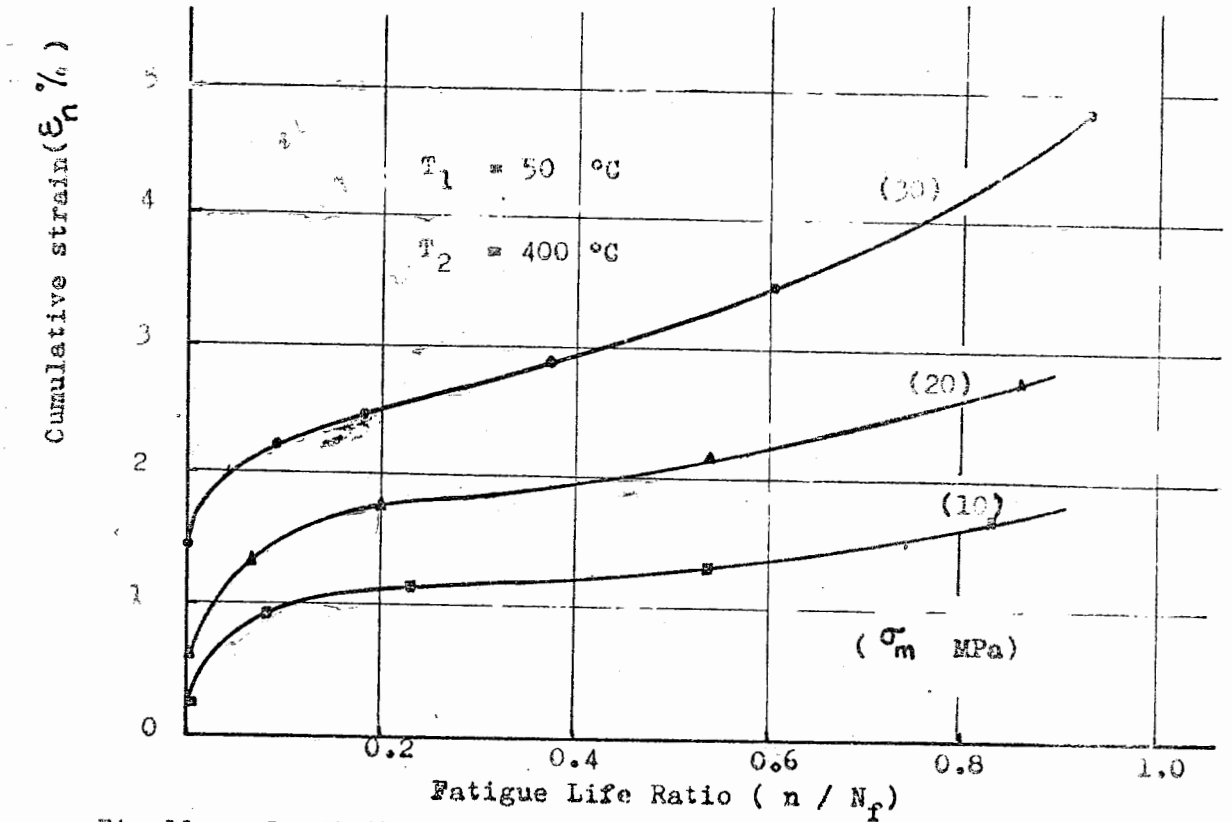

Fig.11: ε_n at thermal cyclic testing for B - samples (σ_m is constant) .

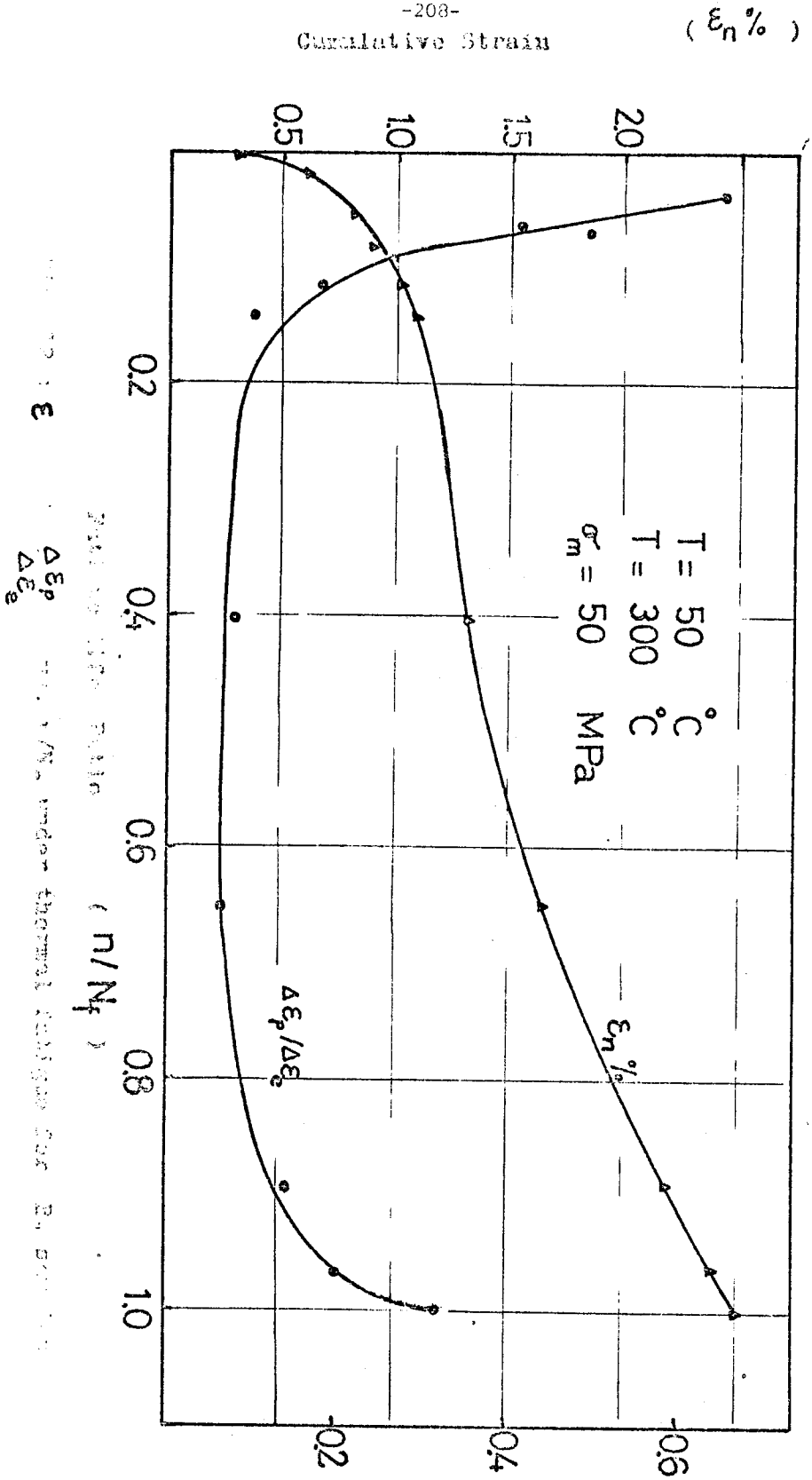

Ratio of palatic strain range to elastic strain range . $(\Delta\varepsilon_p/\Delta\varepsilon_e)$